CrossMark

ORIGINAL RESEARCH ARTICLE

Differentiation of murine models of "negative ERG" by single and repetitive light stimuli

**Naoyuki Tanimoto · James D. Akula · Anne B. Fulton ·
Bernhard H. F. Weber · Mathias W. Seeliger**

Abstract

Purpose Marked attenuation of the single-flash electroretinographic (ERG) b-wave in the presence of a normal-amplitude or less-attenuated a-wave is commonly referred to as the "negative ERG." The purpose of this study was to investigate whether the disparate origins of the negative ERG in three murine models can be discriminated using flickering stimuli.

Methods Three models were selected: (1) the Nyx^{nob} mouse model of complete congenital stationary night blindness, (2) the oxygen-induced retinopathy (OIR) rat model of retinopathy of prematurity (ROP), and (3) the $Rs1$ knockout (KO) mouse model of X-linked juvenile retinoschisis. Directly after a dark-adapted, single-flash ERG luminance series, a flicker ERG frequency series (0.5–30 Hz) was performed at a fixed

luminance of 0.5 log cd s/m². This series includes frequency ranges that are dominated by activity in (A) the rod pathways (below 5 Hz), (B) the cone ON-pathway (5–15 Hz), and (C) the cone OFF-pathway (above 15 Hz).

Results All three models produced markedly attenuated single-flash ERG b-waves. In the Nyx^{nob} mouse, which features postsynaptic deficits in the ON-pathways, the a-wave was normal and flicker responses were attenuated in ranges A and B, but not C. The ROP rat is characterized by inner-retinal ischemia which putatively affects both ON- and OFF-bipolar cell activity; flicker responses were reduced in all ranges (A–C). Notably, the choroid supplies the photoreceptors and is thought to be relatively intact in OIR, an idea supported by the nearly normal a-wave. Finally, in the $Rs1$ KO mouse, which has documented abnormality of the photoreceptor-bipolar synapse affecting both ON- and OFF-pathways, the flicker responses were attenuated in all ranges (A–C). The a-wave was also attenuated, likely as a consequence to schisms in the photoreceptor layer.

Conclusion Consideration of both single-flash and flickering ERG responses can discriminate the functional pathology of the negative ERG in these animal models of human disease.

Keywords Negative electroretinogram · Flicker · Murine model · Complete congenital stationary night blindness (cCSNB) · Retinopathy of prematurity (ROP) · X-linked juvenile retinoschisis (XLRS)

N. Tanimoto (✉) · M. W. Seeliger
Division of Ocular Neurodegeneration, Institute for Ophthalmic Research, Centre for Ophthalmology, Eberhard Karls University, Schleichstr. 4/3, 72076 Tübingen, Germany
e-mail: naoyuki.tanimoto@med.uni-tuebingen.de

J. D. Akula · A. B. Fulton
Department of Ophthalmology, Boston Children's Hospital, 300 Longwood Avenue, Fegan 4, Boston, MA 02115, USA

B. H. F. Weber
Institute of Human Genetics, University of Regensburg, Franz-Josef-Strauss-Allee 11, Regensburg 93053, Germany

🖄 Springer

Introduction

Retinal function can be assessed, noninvasively and objectively, by full-field electroretinograms (ERGs) recorded at the cornea. The single-flash ERG is dominated by two major components: the initial, negative-going a-wave and the subsequent, positive-going b-wave. In normal rodent and primate eyes, the b-wave is generally larger than the a-wave. In some retinal disorders, the b-wave is smaller than the a-wave; the waveform, designated a "negative ERG," is dominated by the negative-going a-wave [1]. The presentation of a negative ERG implies impairment of depolarizing (ON-) bipolar cell signaling or reduction in synaptic transmission from photoreceptors to ON-bipolar cells with a (relative) preservation of rod photoreceptor signaling; it is observed under particular conditions of the retina such as inner-retinal ischemia and synaptic dysfunction between photoreceptors and bipolar cells [2]. For a further differentiation, alternative retinal stimulation protocols are necessary to determine which of these conditions is present in the retina.

One such protocol is the light-adapted, long-flash ERG [3], which permits independent assessment of the cone OFF-pathway. While the long-flash ERG paradigm is effective in primates, it is unfortunately ineffective in mice and rats [4–7]. ERG flicker frequency series at high, fixed luminance (0.5 log cd s/m^2) enables assessment of the major photoreceptor to bipolar cell pathways, *including* the cone OFF-pathway [8]. Therefore, such a protocol is of putative value in determining the cause of the negative ERG.

To determine the effectiveness of this flicker approach, we studied three murine models of three retinal disorders characterized by the negative ERG: (1) the Nyx^{nob} mouse model of complete congenital stationary night blindness (cCSNB), which is one of the two subgroups of CSNB featuring postsynaptic, ON-bipolar cell-specific deficits [9–11], (2) the oxygen-induced retinopathy (OIR) rat model of retinopathy of prematurity (ROP), which is defined by abnormalities in the retinal vasculature [12–15], and (3) the $Rs1$ knockout (KO) mouse model of X-linked juvenile retinoschisis (XLRS), demonstrating a disorganized retina throughout the retinal layers as well as presynaptic abnormalities at the photoreceptor-bipolar synapse [16–18]. We found that, by combining information in single-flash and flicker ERGs, these disease conditions became readily discriminable.

Methods

Ethical approval

All animals were treated in accordance with the ARVO statement for the Use of Animals in Ophthalmic and Vision Research and the law of animal experimentation issued by the German Government. All experimental procedures were approved by the local government authority (Regierungspräsidium Tübingen).

Animals

Electroretinography was performed in five Nyx^{nob} [9] and three control C57BL/6J mice at the age of 6 weeks, in three Long-Evans pigmented ROP rats [15] and four control littermates at the age of 3 weeks, and in five $Rs1$ KO [16] and three control C57BL/6 J mice at the age of 5 months. In ROP rats, OIR was induced by placing newborn pups and dam in an OxyCycler (Biospherix Ltd., Lacona, NY) and exposing them to alternating 24-h periods of 50 and 10 % oxygen starting on the day of birth and lasting for 2 weeks, when they were returned to room air (21 % oxygen). ROP rats were generated in Boston Children's Hospital with the approval by the Animal Care and Use Committee at Children's Hospital Boston, Boston, USA. Littermates were room-air-reared and served as controls. The rats, along with their nursing dam, were shipped overnight for study at the Institute for Ophthalmic Research, Tübingen, Germany.

Electroretinography

ERGs were recorded as previously described [19]. Briefly, animals were dark-adapted longer than 12 h and anesthetized with subcutaneous injection of a mixture of ketamine, xylazine, and physiological saline. For mice, 66.7 mg/kg ketamine and 11.7 mg/kg xylazine were used; for rats, 46.8 mg/kg ketamine and 9.3 mg/kg xylazine were used. The pupils were dilated with tropicamide eye drops (0.5 %; Mydriaticum Stulln, Pharma Stulln, Stulln, Germany). Responses were recorded using custom-made gold wire ring electrodes (Ø of the wire: 0.25 mm)

positioned on the surface of both corneae for binocular ERG recordings. Stainless steel needle electrodes were applied subcutaneously at the middle of the forehead region and the back near the tail as a reference and a ground electrode, respectively. The ERG apparatus consisted of a xenon light source, a Ganzfeld bowl, a signal amplification system (bandpass 0.3–300 Hz), a PC-based control and recording unit, and a monitor (Multiliner Vision; VIASYS Healthcare GmbH, Hoechberg, Germany). Light calibrations were performed using an IL-1700 photometer (International Light, Newburyport, MA, USA). All preparations for ERG recording were done using a portable dim red light source (light-emitting diode, $\lambda > 600$ nm).

Single-flash experiments

Single-flash ERGs were obtained under dark-adapted conditions. Single, xenon stimuli, ranging in luminance from -4 to 1.5 log cd s/m^2, were presented in ten monotonically increasing steps. Ten responses were averaged with interstimulus intervals of 5 s (for -4 to -0.5 log cd s/m^2) or 17 s (for 0–1.5 log cd s/m^2). At the maximal flash luminance of 1.5 log cd s/m^2 where the initial negative-going a-wave is almost saturated and least obscured by the subsequent positive-going b-wave, a-wave amplitude was measured from the prestimulus baseline to the trough of the a-wave.

Flicker experiments

Responses to trains of brief flashes of fixed luminance (0.5 log cd s/m^2) but varying frequency (0.5, 1, 2, 3, 5, 7, 10, 12, 15, 18, 20, and 30 Hz) were obtained [8]. During this recording protocol, no background illumination was used. Flicker responses were averaged either 20 times (for 0.5–3 Hz) or 30 times (for 5 Hz and above) over time, including the first response at each stimulus frequency. All recording parameters were preprogrammed: The inter-recording interval was <5 s, and the whole series was performed within 4 min. Therefore, retinal adaptive state changes in a reproducible way during the recording session. Flicker response amplitude was measured from the trough to the peak of each response. This series includes frequency ranges that are dominated by activity in (A) the rod pathways (below 5 Hz), (B) the cone ON-

pathway (between 5 and 15 Hz), and (C) the cone OFF-pathway (above 15 Hz) which have been confirmed by assessing ERGs in pathway-specific knockout mouse lines [8]. It is noted that cone-driven signals are isolated at 5 Hz and above although no adapting background illumination is used in this flicker protocol. Due to the frequent, repetitive stimuli at the high stimulus luminance of 0.5 log cd s/m^2, the rod-driven signals remain elevated; thus, no additional signals cannot be generated by the rod pathways after each flicker stimulation (our unpublished data, using a modified flicker protocol with a defined onset). Therefore, at 5 Hz and above, no flicker ERG is generated in functionally rod-specific mice, whereas flicker response amplitudes are comparable between wild-type and functionally cone-specific mice [8].

Results

In each murine model, we first assessed dark-adapted, single-flash ERG a- and b-waves for a functional evaluation of outer- and inner-retinal layers, respectively. As we have included "negative ERG" models in this study, a marked attenuation of the single-flash ERG b-wave was expected in each model. Subsequently, flicker ERGs in ranges A–C were evaluated for an assessment of the major vertical photoreceptor–bipolar cell pathways, which could compliment information about layers in the single-flash ERG and allow for a discrimination of an underlying functional pathology.

Nyx^nob mouse

Nyx encodes nyctalopin, which is expressed in the dendritic tips of ON-bipolar cells (both rod and ON-cone) [20] and is indispensable for the proper expression of the effecter channels of the mGluR6 signaling cascade in ON-bipolar cells [21]. The *Nyx*^nob mouse model has a deletion in the *Nyx* gene [10], and due to the deficits of the signaling cascade in the dendritic tips of ON-bipolar cells, each single ON-bipolar cell is not responsive to glutamate puffs [20]. In in vivo ERG, it has been characterized by a lack of single-flash b-wave [9], as the b-wave is generated mainly by ON-bipolar cells [7]. First, we confirmed this phenotype in the single-flash ERG that the b-wave was completely missing (Fig. 1a). In contrast, the a-wave (at
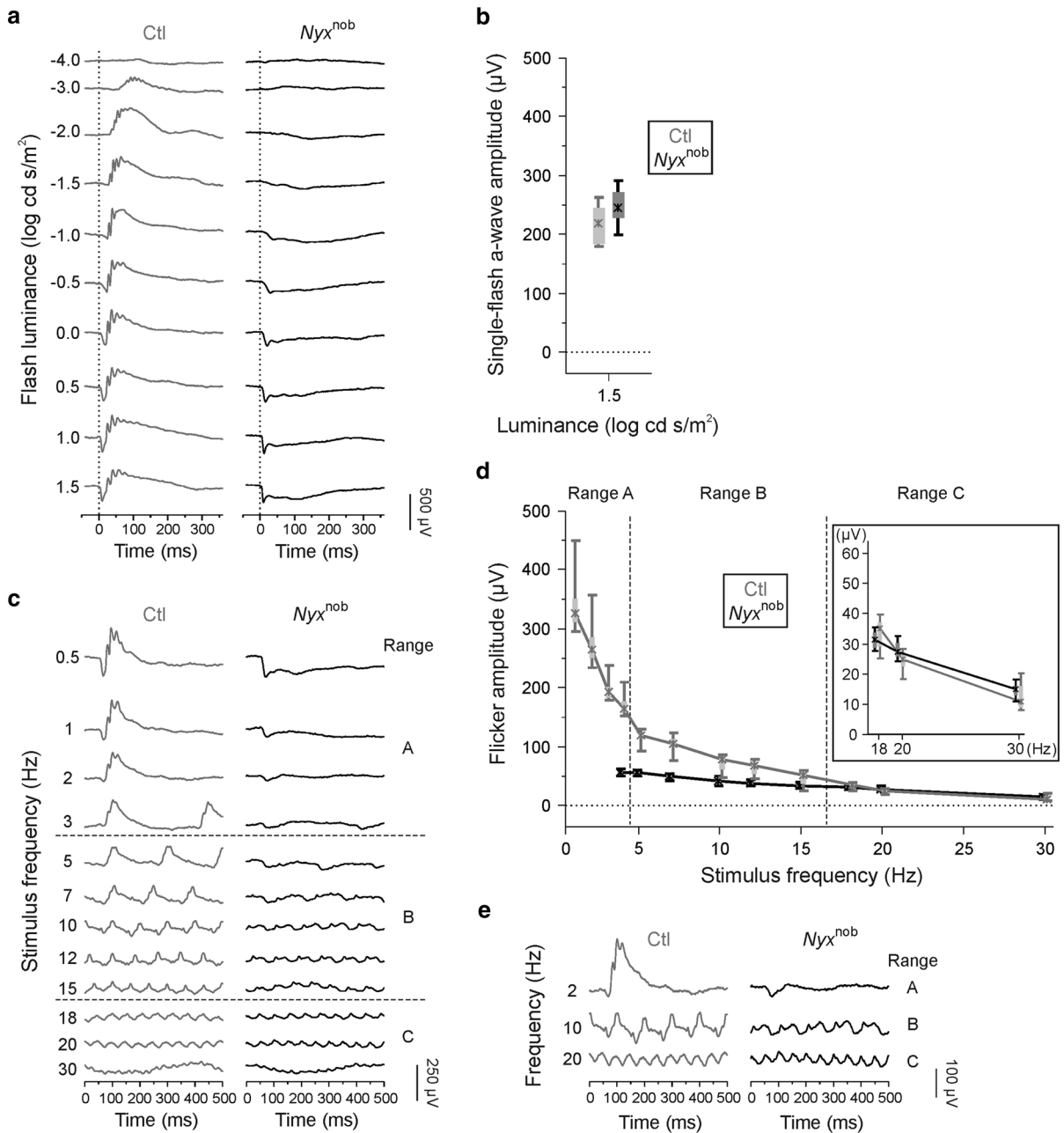
Fig. 1 ERGs in Nyx^{nob} mice. **a** Representative dark-adapted single-flash ERGs in Nyx^{nob} (*black*) and control (Ctl, *gray*) mice. **b** Quantitative evaluation (*box*-and-*whisker plot*, indicating the 5th, 25th, 50th, 75th, and 95th percentiles of the data) of dark-adapted single-flash a-wave amplitudes at 1.5 log cd s/m². **c** Flicker ERGs at 0.5 log cd s/m² recorded from the same mice as in (**a**). **d** *Box*-and-*whisker plot* of flicker response amplitudes. *Inset* in (**d**): Details of the flicker amplitude data of

Nyx^{nob} and Ctl mice at 18, 20, and 30 Hz. **e** Enlargement of the recording traces at 2, 10, and 20 Hz from (**c**). See "Methods" for details of the frequency ranges in (**c**, **d**, **e**). Flicker amplitudes at 0.5, 1, and 2 Hz were not determined in Nyx^{nob} mice because there was no clear positive-going response peak. In Nyx^{nob} mice, the a-wave and the flicker responses in range C were comparable in size to those in control mice

1.5 log cd s/m^2) was not attenuated in Nyx^{nob} mice (Fig. 1a, b), indicating normal functionality of rod photoreceptor outer segments. Thus, the results obtained herein (Fig. 1a, b) were entirely consistent with such a postsynaptic abnormality [9, 20, 21].

In the flicker ERG, the responses in range A were remarkably different in configuration between Nyx^{nob} and control mice, i.e., no clear positive-going response and no oscillations in Nyx^{nob} mice (Fig. 1c). Due to this response configuration, flicker amplitudes were not determined at frequencies below 3 Hz, but it was obvious that the Nyx^{nob} flicker responses were reduced in range A (Fig. 1c, d). In range B, the difference in flicker amplitude between Nyx^{nob} and control mice became smaller as the frequency approached 15 Hz (Fig. 1c, d). The flicker waveform in the Nyx^{nob} mouse lacked prominent positive peak resulting in a "trapezoidal" shape that differed from the "triangular" shape in the control mice (Fig. 1c, e). In range C, however, flicker ERG amplitudes in Nyx^{nob} mice were indistinguishable from those in control mice, likely due to a normally functioning cone OFF-pathway (Fig. 1c–e). These results were in line with previous studies from other laboratories in which flicker ERG properties in Nyx^{nob} mice were analyzed in detail [6, 22]: In flicker ERG, amplitude and phase differences are quite small at around 15–16 Hz and above between control and Nyx^{nob} mice due to the predominant OFF-cone bipolar cell contributions to high-frequency flicker ERGs. Overall, the functional phenotype in Nyx^{nob} mice was comparable to that in $mGluR6$ knockout mice [8], which also features a selective postsynaptic ON-pathway dysfunction [23].

ROP rat

The OIR rat model of ROP is characterized by abnormal retinal vasculature which presumably under-supplies inner-retinal neurons including both ON- and OFF-bipolar cells; the rod photoreceptors, however, would be expected to be less impacted because their oxygen supply derives from the choroid [24]. Correspondingly, in the single-flash ERG, the b-wave was strongly reduced (Fig. 2a). It is noted that the b-wave was not completely abolished at low, scotopic luminance (see −3.0 and −2.0 log cd s/m^2 in Fig. 2a), indicating that there were ON-bipolar cells which could react to signals from photoreceptors. The amplitude of the saturating a-wave (i.e., 1.5 log cd s/m^2

in Fig. 2a) was similar between ROP and the control rats (Fig. 2b). In previous studies, ROP rats (results from larger samples, more commonly studied albinos than the Long-Evans) have shown mild but statistically significant deficits in rod photoreceptor sensitivity [13, 25]. In the human ROP, mild but significant deficits in rod photoreceptor sensitivity are present in infancy and persist many years later [26], and b-wave deficits are present in infancy but disappear later in childhood and adolescence if the ROP had been mild [14]; the 3-week-old OIR rats that we have studied would model the younger end of the age range included in the study of humans [14].

In the flicker ERG, responses were attenuated across all ranges (A–C in Fig. 2c–e), in accordance with ischemia of all inner-retinal cell types. Importantly, a clear difference was observed in range C between ROP rats and Nyx^{nob} mice, demonstrating that ischemic and postsynaptic disease conditions could be discriminated qualitatively in range C of the flicker ERG.

As an aside, while the ERG responses across murine species are remarkably similar, especially with respect to first (rod)- and second (bipolar)-order neurons, we do recognize that the mouse and rat ERGs have subtle difference [7].

$Rs1$ KO mouse

Retinoschisin plays an essential role in the maintenance of the retinal structure [17], and $Rs1$ KO retina is disorganized throughout, including the photoreceptor and bipolar cell layers; there is a slow, but progressive, photoreceptor degeneration [16, 27]. In single-flash ERG, the amplitudes of both the a- and b-waves were noticeably attenuated (Fig. 3a, b), but, importantly, the b-wave was *more* attenuated than the a-wave, resulting in a negative ERG at the highest flash luminance examined (1.5 log cd s/m^2 in Fig. 3a; the % attenuation of the b-wave in $Rs1$ KO mice was 63.8 %, whereas that of the a-wave was 55.2 %). This single-flash ERG phenotype can be explained by presynaptic abnormalities at the photoreceptor-bipolar synapse [17, 18], leading to reduced transmission between photoreceptors and bipolar cells. Additionally, morphological alterations are distributed neither evenly nor regularly but rather in a mottled pattern [16]; therefore, the alterations do not always present in the same "vertical" column. Consequently, the
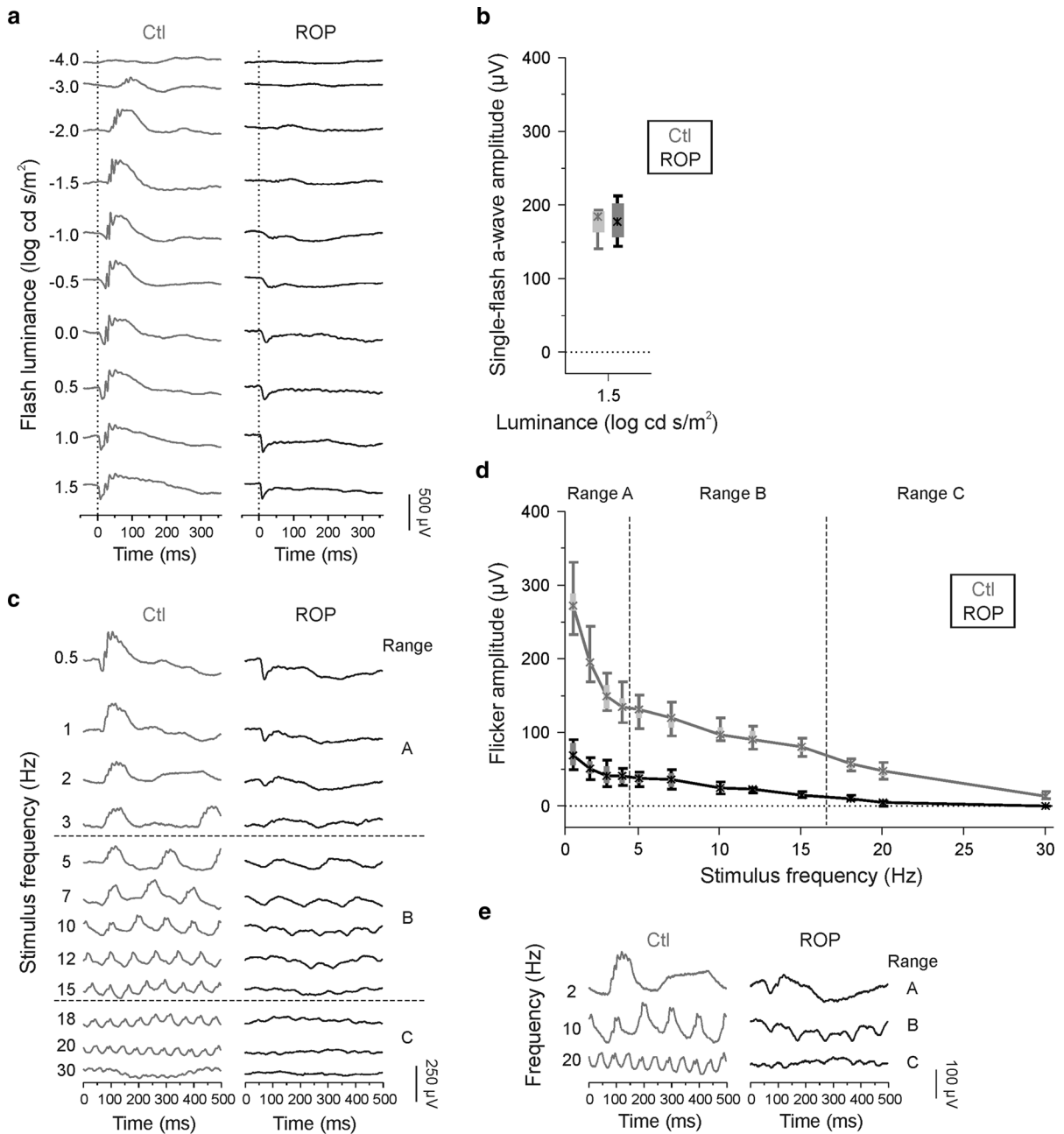
Fig. 2 ERGs in ROP rats. **a** Representative dark-adapted single-flash ERGs in ROP (*black*) and control (Ctl, *gray*) rats. **b** Quantitative evaluation (*box-and-whisker plot*, indicating the 5th, 25th, 50th, 75th, and 95th percentiles of the data) of dark-adapted single-flash a-wave amplitudes at 1.5 log cd s/m². **c** Flicker ERGs at 0.5 log cd s/m² recorded from the same rats as in (**a**). **d** *Box-and-whisker plot* of flicker response amplitudes. **e** Enlargement of the recording traces at 2, 10, and 20 Hz from (**c**). See "Methods" for details of the frequency ranges in (**c, d, e**). In ROP rats, the a-wave was not substantially affected, whereas flicker responses were reduced in all three frequency ranges

fraction of functional photoreceptors may exceed that of functional bipolar cells receiving photoreceptor inputs. These reasons, which are not mutually exclusive, presumably explain why *Rs1* KO mice show stronger attenuation of the b-wave than the a-wave.
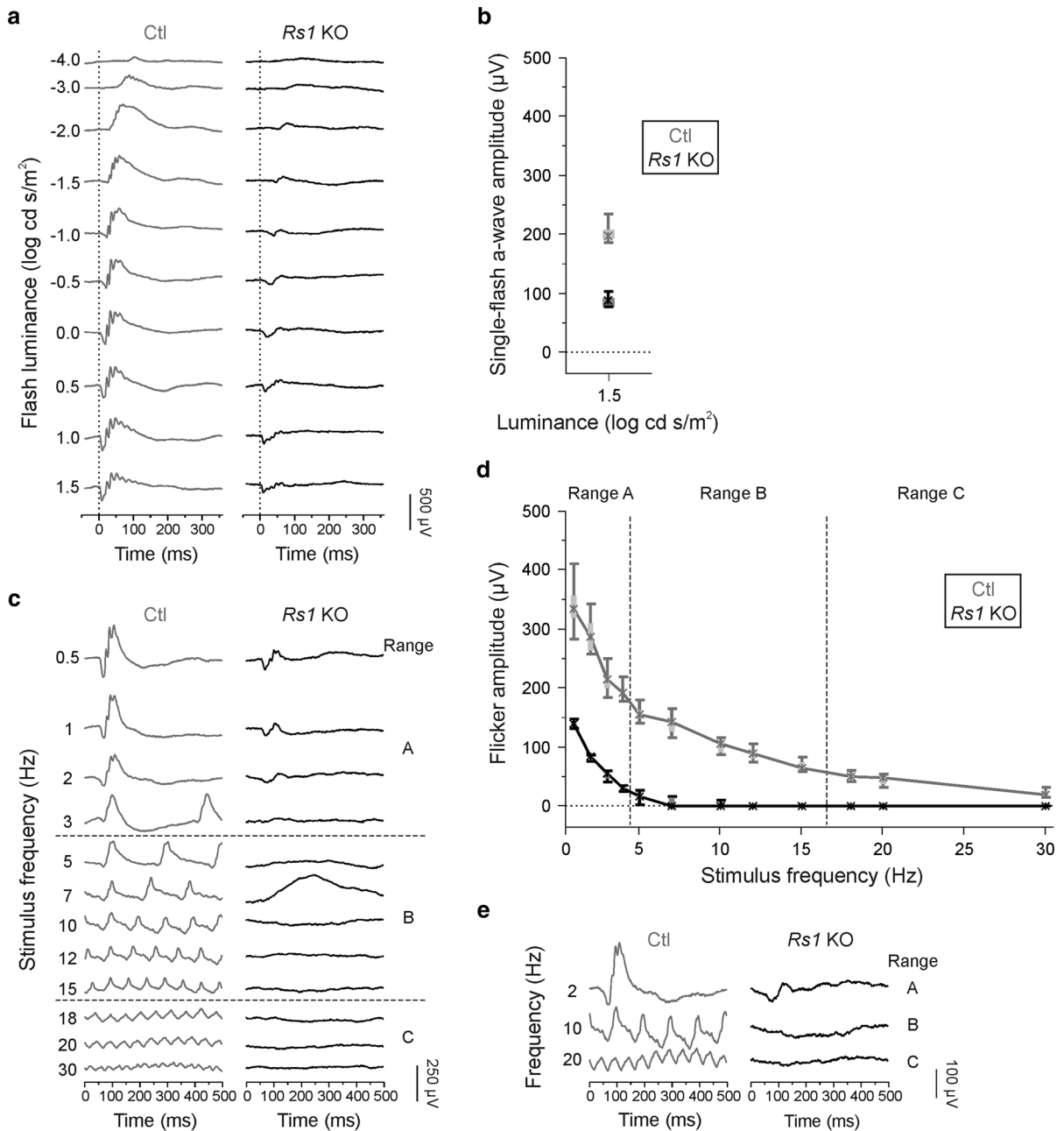
Fig. 3 ERGs in *Rs1* knockout (KO) mice. **a** Representative dark-adapted single-flash ERGs in *Rs1* KO (*black*) and control (Ctl, *gray*) mice. **b** Quantitative evaluation (*box-and-whisker plot*, indicating the 5th, 25th, 50th, 75th, and 95th percentiles of the data) of dark-adapted single-flash a-wave amplitudes at 1.5 log cd s/m². **c** Flicker ERGs at 0.5 log cd s/m² recorded

from the same mice as in (**a**). **d** *Box*-and-*whisker plot* of flicker response amplitudes. **e** Enlargement of the recording traces at 2, 10, and 20 Hz from (**c**). See "Methods" for details of the frequency ranges in (**c**, **d**, **e**). In *Rs1* KO mice, the a-wave as well as the flicker responses in all three frequency ranges were attenuated

In the flicker ERG, responses in *Rs1* KO mice were strongly reduced at all stimulus frequencies examined (Fig. 3c–e), consistent with the nonspecific irregular

alterations in the *Rs1* KO retina [16] affecting rod bipolar cells and ON- and OFF-cone bipolar cells. In this regard, the nonselective reduction in flicker ERGs

Table 1 Summary of in vivo functional data

Negative ERG model	Single-flash ERG a-wave[a]	Flicker ERG		
		Range A	Range B	Range C
Nyx[nob] mouse	→	↓	↓	→
ROP rat	→	↓	↓	↓
Rs1 KO mouse	↓	↓	↓	↓

"→" No substantial reduction, "↓" reduced, *ERG* electroretinogram, *KO* knockout, *ROP* retinopathy of prematurity

[a] At 1.5 log cd s/m^2 stimulus luminance

in *Rs1* KO mice was similar to ROP rats. However, unlike in the ROP rats, the a-wave was reduced in *Rs1* KO mice due to disruption of the photoreceptors (Fig. 3a, b).

It is noted that there are some interspecies differences in disease pathology; the models are, as always, imperfect. For example, the negative ERG phenotype is common in both *Rs1* KO mice and patients with XLRS [16, 28], but there are some differences in single-flash ERG a-wave and flicker ERGs: Whereas both response components were remarkably reduced in *Rs1* KO mice (Fig. 3), in patients with XLRS, both a-wave and fast flicker responses are well preserved in many cases [28].

Discussion

In this study, three murine models of eye disease (cCSNB, ROP, and XLRS), all featuring a negative ERG waveform, were readily discriminated by the results of ERG responses to single flash and to flickering stimuli. The three models have distinct sites of dysfunction and presented three distinct patterns in ERG parameter changes (Table 1). Notably, the ERG changes expected from the recognized pathology of each disease model aligned nearly perfectly with the observed results, inspiring confidence that this approach has diagnostic utility.

Among the parameters analyzed in this study, the a-wave at 1.5 log cd s/m^2 and the flicker responses in range C (above 15 Hz) are together determinative for discrimination of the models under study (Table 1). Since the amplitude of the a-wave and the flicker responses in range C can be quickly surveyed by the ERG, this diagnostic strategy might form part of a useful nosology in negative ERG cases of unknown

etiology at the beginning of a study, e.g., [29]. For example, a negative ERG in the presence of a regular a-wave and normal flicker ERGs in range C may lead to presumption of a postsynaptic ON-pathway disorder. Or, a normal a-wave and attenuated b-wave in the presence of attenuated flicker responses at all frequencies might prompt an inspection of the retinal vessels by angiography. In this way, further targeted investigations may be smoothly and optimally planned in the same animals to elucidate etiology, such as in vivo morphological examinations, genetic analysis, and ex vivo experiments on function and morphology.

References

1. Karpe G (1946) The basis of clinical electroretinography. Acta Ophthalmol 24(Suppl):5–118
2. Pardue MT, Peachey NS (2014) Mouse b-wave mutants. Doc Ophthalmol 128:77–89
3. Audo I, Robson AG, Holder GE, Moore AT (2008) The negative ERG: clinical phenotypes and disease mechanisms of inner retinal dysfunction. Surv Ophthalmol 53:16–40
4. Xu L, Ball SL, Alexander KR, Peachey NS (2003) Pharmacological analysis of the rat cone electroretinogram. Vis Neurosci 20:297–306
5. Sharma S, Ball SL, Peachey NS (2005) Pharmacological studies of the mouse cone electroretinogram. Vis Neurosci 22:631–636
6. Shirato S, Maeda H, Miura G, Frishman LJ (2008) Postreceptoral contributions to the light-adapted ERG of mice lacking b-waves. Exp Eye Res 86:914–928
7. Frishman LJ, Wang MH (2011) Electroretinogram of human, monkey and mouse. In: Levin LA, Nilsson SF, Ver Hoeve J, Wu SM, Kaufman PL, Alm A (eds) Adler's physiology of the eye, 11th edn. Saunders Elsevier, New York, pp 480–501
8. Tanimoto N, Sothilingam V, Kondo M, Biel M, Humphries P, Seeliger MW (2015) Electroretinographic assessment of rod- and cone-mediated bipolar cell pathways using flicker stimuli in mice. Sci Rep 5:10731
9. Pardue MT, McCall MA, LaVail MM, Gregg RG, Peachey NS (1998) A naturally occurring mouse model of X-linked congenital stationary night blindness. Invest Ophthalmol Vis Sci 39:2443–2449
10. Gregg RG, Mukhopadhyay S, Candille SI, Ball SL, Pardue MT, McCall MA, Peachey NS (2003) Identification of the gene and the mutation responsible for the mouse nob phenotype. Invest Ophthalmol Vis Sci 44:378–384
11. Zeitz C, Robson AG, Audo I (2015) Congenital stationary night blindness: an analysis and update of genotype-phenotype correlations and pathogenic mechanisms. Prog Retin Eye Res 45:58–110
12. Penn JS, Tolman BL, Lowery LA (1993) Variable oxygen exposure causes preretinal neovascularization in the newborn rat. Invest Ophthalmol Vis Sci 34:576–585
13. Liu K, Akula JD, Falk C, Hansen RM, Fulton AB (2006) The retinal vasculature and function of the neural retina in a rat model of retinopathy of prematurity. Invest Ophthalmol Vis Sci 47:2639–2647
14. Harris ME, Moskowitz A, Fulton AB, Hansen RM (2011) Long-term effects of retinopathy of prematurity (ROP) on rod and rod-driven function. Doc Ophthalmol 122:19–27
15. Favazza TL, Tanimoto N, Munro RJ, Beck SC, Garcia Garrido M, Seide C, Sothilingam V, Hansen RM, Fulton AB, Seeliger MW, Akula JD (2013) Alterations of the tunica vasculosa lentis in the rat model of retinopathy of prematurity. Doc Ophthalmol 127:3–11
16. Weber BH, Schrewe H, Molday LL, Gehrig A, White KL, Seeliger MW, Jaissle GB, Friedburg C, Tamm E, Molday RS (2002) Inactivation of the murine X-linked juvenile retinoschisis gene, Rs1h, suggests a role of retinoschisin in retinal cell layer organization and synaptic structure. Proc Natl Acad Sci USA 99:6222–6227
17. Molday RS, Kellner U, Weber BH (2012) X-linked juvenile retinoschisis: clinical diagnosis, genetic analysis, and molecular mechanisms. Prog Retin Eye Res 31:195–212
18. Shi L, Jian K, Ko ML, Trump D, Ko GY (2009) Retinoschisin, a new binding partner for L-type voltage-gated calcium channels in the retina. J Biol Chem 284:3966–3975
19. Tanimoto N, Sothilingam V, Seeliger MW (2013) Functional phenotyping of mouse models with ERG. Methods Mol Biol 935:69–78
20. Gregg RG, Kamermans M, Klooster J, Lukasiewicz PD, Peachey NS, Vessey KA, McCall MA (2007) Nyctalopin expression in retinal bipolar cells restores visual function in a mouse model of complete X-linked congenital stationary night blindness. J Neurophysiol 98:3023–3033
21. Pearring JN, Bojang P Jr, Shen Y, Koike C, Furukawa T, Nawy S, Gregg RG (2011) A role for nyctalopin, a small leucine-rich repeat protein, in localizing the TRP melastatin 1 channel to retinal depolarizing bipolar cell dendrites. J Neurosci 31:10060–10066
22. Krishna VR, Alexander KR, Peachey NS (2002) Temporal properties of the mouse cone electroretinogram. J Neurophysiol 87:42–48
23. Masu M, Iwakabe H, Tagawa Y, Miyoshi T, Yamashita M, Fukuda Y, Sasaki H, Hiroi K, Nakamura Y, Shigemoto R, Takada M, Nakamura K, Nakao K, Katsuki M, Nakanishi S (1995) Specific deficit of the ON response in visual transmission by targeted disruption of the mGluR6 gene. Cell 80:757–765
24. Cringle SJ, Yu DY, Alder VA (1991) Intraretinal oxygen tension in the rat eye. Graefes Arch Clin Exp Ophthalmol 229:574–577
25. Akula JD, Hansen RM, Martinez-Perez ME, Fulton AB (2007) Rod photoreceptor function predicts blood vessel abnormality in retinopathy of prematurity. Invest Ophthalmol Vis Sci 48:4351–4359
26. Fulton AB, Hansen RM, Moskowitz A, Akula JD (2009) The neurovascular retina in retinopathy of prematurity. Prog Retin Eye Res 28:452–482
27. Janssen A, Min SH, Molday LL, Tanimoto N, Seeliger MW, Hauswirth WW, Molday RS, Weber BH (2008) Effect of late-stage therapy on disease progression in AAV-mediated rescue of photoreceptor cells in the retinoschisin-deficient mouse. Mol Ther 16:1010–1017
28. Vincent A, Robson AG, Neveu MM, Wright GA, Moore AT, Webster AR, Holder GE (2013) A phenotype-genotype correlation study of X-linked retinoschisis. Ophthalmology 120:1454–1464
29. Balmer J, Ji R, Ray TA, Selber F, Gassmann M, Peachey NS, Gregg RG, Enzmann V (2013) Presence of the Gpr179(nob5) allele in a C3H-derived transgenic mouse. Mol Vis 19:2615–2625